

Laser-induced birefringence in a wavelength-mismatched cascade system of inhomogeneously broadened Yb atoms

Tai Hyun Yoon,* Chang Yong Park, and Sung Jong Park

Center for Optical Frequency Control, Korea Research Institute of Standards and Science, 1 Doryong, Yuseong, Daejeon 305-340, Korea

(Received 22 July 2004; revised manuscript received 24 September 2004; published 14 December 2004)

We report the observation of laser-induced birefringence (LIB) in a wavelength-mismatched cascade system ($J=0 \leftrightarrow J=1 \leftrightarrow J=0$ transitions) of inhomogeneously broadened ytterbium atoms with strong pump and probe fields. We investigate the transmission spectrum of two circular polarization (σ_p^+ and σ_p^-) components of strong probe field at fixed frequency, depending on the detuning of a circularly polarized (σ_c^-) coupling field from two-photon resonance. We find that the σ_p^+ (σ_p^-) polarized component exhibits a narrow electromagnetically induced absorption (transparency) spectrum. Numerical solutions of density matrix equations show qualitative agreement with experimental results. A Doppler-free dispersive LIB signal is obtained by detecting the Stokes parameter of the probe field, enabling us to stabilize the frequency of the coupling laser without frequency modulation.

DOI: 10.1103/PhysRevA.70.061803

PACS number(s): 42.62.Fi, 32.80.Pj, 39.25.+k

Quantum coherence effects in atomic three-level systems interacting with two monochromatic laser fields provide a rich source of interesting phenomena in laser spectroscopy, such as, the phenomena of electromagnetically induced transparency (EIT) and absorption (EIA) [1], etc. Complete coherent control of the polarization state of an optical field [2], measurement of the optical rotation to investigate the atomic parity nonconservation in thallium vapor [3], and measurement of birefringence at 1083 nm in ^4He atoms [4] have been achieved relying on the EIT effects in the corresponding cascade three-level atomic systems. Recently, Magno and co-worker [5] proposed a simple scheme for laser cooling of alkaline-earth and ytterbium atoms using a two-photon $^1S_0 \leftrightarrow ^1P_1 \leftrightarrow ^1S_0$ cascade transition, which might be used as a second stage cooling after precooling with the $^1S_0 \rightarrow ^1P_1$ transition, and this two-photon laser cooling scheme has not been realized yet experimentally.

In this paper, we present a Doppler-free two-photon atomic coherence spectroscopy of Yb atoms associated with the wavelength-mismatched cascade scheme considered in the two-photon cooling of Yb atoms [5]. We investigate the Doppler-free transmission spectrum of two circular polarization (σ_p^+ and σ_p^-) components of a strong probe field at fixed detuning from a one-photon resonance in a Yb hollow cathode lamp (HCL) depending on the detuning of circularly polarized (σ_c^-) counterpropagating coupling field from two-photon resonance. We find that when the Rabi frequencies of the probe and coupling fields are similar to the decay rate of the $J=1$ state, the σ_p^+ component exhibits a narrow EIA spectrum, while the σ_p^- component exhibits an EIT spectrum due to the multiphoton process induced via the strong probe field. The measured spectra show qualitative agreement with the calculated spectra from numerical solutions of semiclassical density matrix equations. A sensitive Doppler-free dispersive signal that is proportional to the birefringence experienced by the two circular polarization components of the probe

field is then subsequently obtained by detecting the Stokes parameter [6] of the transmitted probe field. This is a measurement of the electromagnetically induced birefringence originating from the EIA-type resonance of the strong probe field in the wavelength-mismatched three-level cascade system. We are able to stabilize the frequency of coupling laser at 1077 nm by use of the laser-induced birefringence (LIB) signal with long-term stability below 1 MHz, which is stable enough to study the two-photon laser cooling of Yb atoms in a Yb magneto-optical trap (MOT) [7].

Figures 1(a) and 1(b), respectively, show the three-level cascade scheme of Yb atoms having m -degenerate sublevels $|2\rangle$ and $|3\rangle$ relevant to the present study and the schematic diagram of the experimental setup. In Fig. 1(a), levels $|1\rangle$, $|2\rangle$, and $|4\rangle$ form a three-level cascade wavelength-mismatched configuration and levels $|2\rangle$ and $|3\rangle$ are coupled to the ground state $|1\rangle$ by an arbitrarily intense probe field. Here we ignore the state with $m_j=0$ of the 1P_1 state for simplicity, but include it for the numerical calculation (see later) [8]. In parentheses on Fig. 1(a), laser frequency, polarization state, and Rabi frequency of the driving fields are

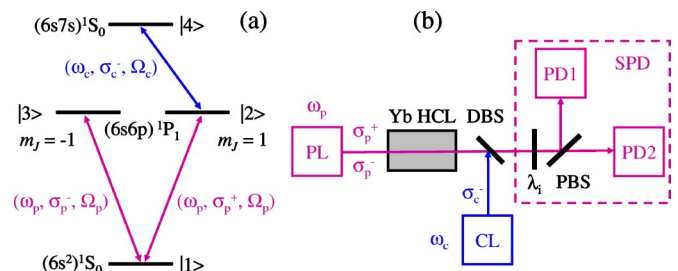


FIG. 1. (a) The three-level cascade scheme of Yb atoms having m -degenerate sublevels $|2\rangle$ and $|3\rangle$. In parentheses, laser frequency, polarization state, and Rabi frequency of the driving fields are explicitly shown. (b) Experimental setup for Doppler-free two-photon atomic coherence spectroscopy. PL, probe laser; CL, coupling laser; SPD, Stokes parameter detector; PD, photodiode; PBS, polarization beam splitter; DBS, dichroic beam splitter; HCL, hollow cathode lamp; λ_i , λ/i waveplate ($i=2,4$).

*Electronic address: thyoan@kriss.re.kr

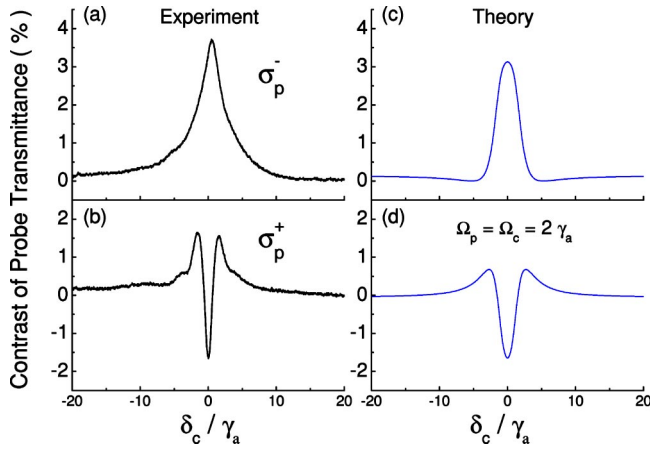


FIG. 2. Measured contrast against the Doppler background of the strong probe field transmittance for the (a) σ_p^- and (b) σ_p^+ components vs δ_c/γ_a at probe and coupling powers of $85 \mu\text{W}$ and 1.7 mW , respectively. The graphs in (c) and (d) are, respectively, the calculated contrasts against Doppler background of probe transmittance for the σ_p^- and σ_p^+ components with the parameters of $\Omega_p = \Omega_c = 2\gamma_a$. In all graphs, we set $\delta_p = 0$.

shown explicitly. The 1P_1 state (levels $|2\rangle$ and $|3\rangle$) decays rapidly with a decay rate of $\gamma_a = 2\pi \times 28 \text{ MHz}$ to level $|1\rangle$ and there is a weak decay channel to the $(6s6p)^3P_1$ state via levels $(6s5d)^3D_1$ and 3D_2 (not shown). The 3P_1 state decays to the ground state by emitting 556 nm spontaneous photons with a decay rate of $2\pi \times 182 \text{ kHz}$. Level $|4\rangle$ decays predominantly to the 1P_1 state with a decay rate of $\gamma_b = 2\pi \times 3.0 \text{ MHz}$ and weakly to the 3P_1 state with a decay rate of $2\pi \times 0.2 \text{ MHz}$ [9].

Note that in the Yb cascade three-level configuration in Fig. 1(a), where $\omega_p \sim 2.7 \times \omega_c$, the effects of mismatching wavelength in the EIT spectrum in Doppler-broadened media is expected to be very strong [10], i.e., the depth of the EIT dip is greatly reduced from the complete transparency as opposed to the case when $\omega_p = \omega_c$ [11] and $\omega_c \sim 1.5 \times \omega_p$ [4]. In this case, the Autler-Townes components for nonzero velocity atoms are completely overlapped with the line center, as opposed to the case when $\omega_p \leq \omega_c$; thus one would reasonably expect transparency created on resonance to be obscured [10]. This is exactly what happens in the cascade system of Fig. 1(a) and observed in Fig. 2 below, where we could detect only a few percent contrast of EIT or EIA signals against the Doppler profile, only when the Rabi frequencies of probe and coupling fields are an order of the decay rate of the $J=1$ state.

Theoretical analysis of the LIB in the same level configuration as in Fig. 1 was discussed previously by Patnaik and Agarwal [8] at the *weak* probe-field limit and wavelength-matched configuration, i.e., $\omega_p = \omega_c$. We find, however, that in the wavelength-mismatched and inhomogeneously broadened cascade configuration, where $\omega_p \gg \omega_c$ as in Ca, Sr, and Yb atoms (considered in the two-photon cooling theory [5]), the LIB signal becomes negligibly small after Doppler averaging [10] when the probe field is weak. Thus, we cannot use the analytical results discussed in Ref. [8] for the explanation of our experimental findings. In this paper, we demonstrate

that if the probe field is *strong* in this level configuration, two circular polarization components of the probe field exhibit an EIA in the σ_p^+ component that is coupled to the control field and EIT in the σ_p^- component that is decoupled from the control field, allowing us to measure the laser-induced birefringence originating from the EIA-type resonance. This is an observation of an electromagnetically induced birefringence associated with the EIA and EIT effects of the strong probe field in the cascade three-level system.

In the experiment, two laser diodes with external grating feedback are used for the probe laser (PL) and coupling laser (CL), respectively, as indicated in Fig. 1(b). The atomic temperature in a Yb HCL is estimated to be $\sim 600 \text{ K}$, which gives a Doppler width of $\sim 1 \text{ GHz}$ [12]. The frequency of probe laser at 399 nm can be stabilized within the range of probe detuning $|\delta_p| < 2\gamma_a \sim 60 \text{ MHz}$ by use of a Doppler-free saturation absorption signal with a lock-in detection using a separate Yb HCL. The two-photon Doppler cancellation, although it is not perfect (since $\omega_p \neq \omega_c$), is achieved with counterpropagating geometry of the coupling and probe fields as in Fig. 1(b). We set the powers of the probe and coupling fields at $P_p = 85 \mu\text{W}$ (spot size $67 \mu\text{m}$, $\Omega_p \sim 2\gamma_a$ for σ_p^+ and σ_p^- components) and $P_c = 1.7 \text{ mW}$ (spot size $175 \mu\text{m}$, $\Omega_c \sim 4\gamma_a$), and the probe field detuning at exact one-photon resonance ($\delta_p = 0$).

We first measured the transmittance spectrum corresponding to the two circularly polarized components of the probe field as a function of coupling field detuning δ_c/γ_a . For this measurement, we used two detectors (PD1 and PD2) in Fig. 1(b) and a $\lambda/4$ wave plate oriented at 45° to the polarization beam splitter (PBS). The first column in Fig. 2 shows the typical transmission spectrum expressed as a contrast against Doppler background (70% absorption) corresponding to the σ_p^- component in (a) and to the σ_p^+ component in (b) for the ^{174}Yb isotope in a Yb HCL with Ne buffer gas (discharge voltage 160 V and current 1.8 mA) [7]. As one can see, the spectrum in (a) corresponds to the σ_p^- component and shows an EIT spectrum with a line width of $\sim 3\gamma_a$, while the spectrum in (b) corresponding to the σ_p^+ component, shows a narrower ($\sim \gamma_a$) EIA spectrum at the two-photon resonance. Note that the EIT and EIA spectrum has only a few percent contrast against Doppler background, which is expected theoretically for the wavelength-mismatched cascade system with $\omega_p \gg \omega_c$ [10]. We also find that, as decreasing the intensity of coupling field, the EIA spectrum in (b) develops into the EIT spectrum as in (a) with a reduced signal-to-noise ratio. However, the σ_p^- component, which is decoupled from the strong control field, always exhibits an EIT spectrum under the parameter range we have tested. The EIT spectrum has a line width about $87 \text{ MHz} \sim 3\gamma_a$, which is 1.5 times larger than the width measured at the Doppler-free saturation absorption spectroscopy with a same Yb HCL due to the saturation broadening [7], while the EIA spectrum has a much more narrow linewidth of about γ_a . We calibrated the width of the measured spectrum from the known frequency interval (isotope shift) of the $^1S_0 - ^1P_1$ transition of Yb isotopes [13]. The narrow feature of the EIA spectrum may be understood that in the EIA process, a higher-order multipath interference is involved compared to the EIT process, since the probe field is strong [11].

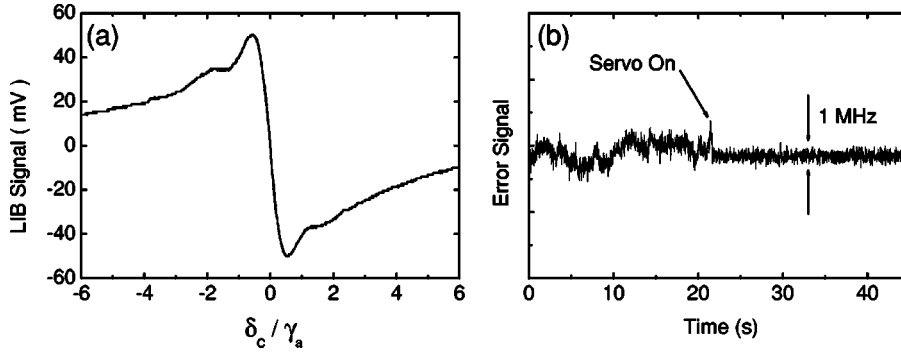


FIG. 3. (a) Doppler-free dispersive LIB signal measured by the SPD in Fig. 1(b). (b) Frequency fluctuation of the coupling laser before and after the servo-loop is on for frequency stabilization.

In order to understand theoretically the measured spectra in Figs. 2(a) and 2(b), we solved a semiclassical density matrix equation associated with the level configuration of Fig. 1(a) at the steady state. The equation of motion for the slowly varying components ρ of the density matrix $\tilde{\rho}$ may be written by making a transformation $\tilde{\rho} \rightarrow \rho$ such that $\rho_{kk} = \tilde{\rho}_{kk}$, $\rho_{ll} = \tilde{\rho}_{ll} \exp(-i\omega_p t)$, $\rho_{4l} = \tilde{\rho}_{4l} \exp(-i\omega_c t)$, $l=2, o, 3$, $\rho_{41} = \tilde{\rho}_{41} \exp[-i(\omega_p + \omega_c)t]$, where subscript o indicates the state with $m=0$ of the 1P_1 level. The matrix equation for ρ is then found to be [8]

$$\dot{\rho} = -\frac{i}{\hbar}[H, \rho] - \sum_{i=2,o,3} (\gamma_b/6\{ |4\rangle\langle 4|, \rho \} + \gamma_a/2\{ |i\rangle\langle i|, \rho \} - \gamma_b \rho_{44} |i\rangle\langle i| - \gamma_a \rho_{ii} |1\rangle\langle 1|), \quad (1)$$

with the effective Hamiltonian in the rotating frame

$$H = \hbar(\delta_p + \delta_c) |4\rangle\langle 4| + \hbar \delta_p \sum_{i=2,3} |i\rangle\langle i| - \frac{\hbar}{2} \sum_{i=2,3} (\Omega_p |i\rangle\langle 1| + \Omega_c |4\rangle\langle 2| + \text{H.c.}). \quad (2)$$

The second term under the summation sign of Eq. (1) represents the natural decays of the system and the curly bracket represents the anticommutator.

The second column in Figs. 2(c) and 2(d) shows the calculated transmission spectrum of the probe field after Doppler averaging expressed as a contrast against Doppler background as a function of δ_c/γ_a with the parameters $\Omega_p = \Omega_c = 2\gamma_a$. The calculated contrast of the probe field transmittance against Doppler background was obtained from the imaginary part of the atomic coherence, i.e., $\text{Im}[\rho_{31}]$ for the σ_p^- component and $\text{Im}[\rho_{21}]$ for the σ_p^+ component. The spectrum in (c) shows an EIT spectrum as in (a), while the spectrum in (d), corresponding to the σ_p^+ component, shows an EIA spectrum as in (b) at the same parameters. The EIA spectrum of the σ_p^+ component of the probe field can be understood as a result of higher-order multiphoton interference enabled by the strong probe field [11]. In addition, our experimental and numerical observations suggest that the σ_p^- component, which is blind to the coupling field, is also actually strongly coupled to the σ_c^- coupling field due to the multiphoton process induced via the strong probe field so that the EIT spectrum is observed.

Although, as one can find, the experimental and theoretical spectra in Fig. 2 agree well qualitatively, there are sig-

nificant differences in line shape. We attribute this difference partly to the unknown discharge effects in the Yb HCL and partly to the uncontrollable imperfections of the polarization elements in the experimental setup. However, we can reasonably say that the density matrix equations in Eqs. (1) and (2) correctly describe the general behavior of the atomic coherence associated with the three-level cascade system with m -degenerate sublevels as in Fig. 1(a). We want to emphasize that at the parameter range where $\Omega_p \ll \gamma_a$ and $\Omega_c \sim \gamma_a$, the calculated transmittances for both σ_p^+ and σ_p^- components exhibit white (flat) spectrum after the Doppler averaging; thus there is no detectable EIT or EIA signals as contrary to the case when $\Omega_p \sim \Omega_c \sim \gamma_a$ as in Fig. 2, strongly supporting our observations. Therefore, it is a very important experimental and theoretical observation that only when the intensity of the probe field and coupling fields are strong, i.e., $\Omega_p \sim \Omega_c \sim \gamma_a$, the transmittances of the σ_p^+ and σ_p^- components in the wavelength-mismatched cascade system exhibit an enhanced absorption or transmittance induced by the narrow two-photon coherence, resulting in the enhancement of laser-induced birefringence, as clearly demonstrated in Fig. 3(a) below.

Strong coupling and probe fields, when applied to an initially isotropic medium containing Yb atoms having m -degenerate sublevels, can create birefringence in the medium. Because, as clearly seen in Fig. 2, the strong driving fields create asymmetry between the susceptibilities χ^\pm of the probe field, since $\chi^{+(-)} = (2\mu/\epsilon_0 E_p) \rho_{21(31)}$, where μ is the dipole matrix element between the 1S_0 - 1P_1 transition, ϵ_0 is the permittivity, and E_p is the amplitude of the probe field. That results in the LIB, i.e., the plane of polarization is rotated when it passes through the medium. For a small absorption, the rotation angle $\Delta\theta$ is given by [6,8]

$$\Delta\theta = \pi k_p L (\chi^+ - \chi^-) = \Delta n k_p L / 2, \quad (3)$$

where k_p corresponds to propagation vector of the probe field, L is length of the cell along k_p , $\Delta n = n^+ - n^-$, $n^\pm = n^\pm + i\alpha^\pm = \sqrt{1 + 4\pi\chi^\pm}$, and n^\pm (α^\pm) being the refractive index (absorption coefficient). Using the numerical solutions for χ_p^\pm from Eqs. (1) and (2), the rotation of polarization $\Delta\theta$ of the probe can easily be determined from Eq. (3). In order to detect the background-free dispersive LIB signal experimentally, we used the Stokes parameter detector (SPD) in Fig. 1(b). In this case, the SPD consists of a $\lambda/2$ wave plate and a balanced polarimeter [6]. The conventional way to measure the polarization state after passing through the medium is to put a

linear polarizer in front of a detector and measure the projected intensity. But, in that case, it is inevitable to include the effect of circular dichroism in addition to the rotation of the polarization axis. In the SPD scheme, however, the $\lambda/2$ wave plate rotates the polarization axis of the probe beam by 45° , and the balanced detector (polarimeter) which subtracts the reflected and transmitted intensities from the PBS measures only the rotation of the polarization axis, i.e., the LIB signal, which is linear in $\Delta\theta$, without background as long as $\Delta\theta \ll 1$ for an optically thin sample, where $\alpha L \ll 1$ [6].

Figure 3(a) shows the detected LIB signal at the same parameter condition as in Fig. 2. The LIB signal has two distinct features originated from the absorption (dispersion) spectrum of the σ_p^+ and σ_p^- components. The narrow dispersion feature at the line center with linewidth about $\sim\gamma_a$ corresponds to the LIB associated with the EIA signal observed for the σ_p^+ component in Fig. 2(b), while the somewhat broad ($\sim 3\gamma_a$) and weak dispersion signal superimposed on the main LIB signal corresponds to the LIB associated with the EIT signal observed for the σ_p^- component in Fig. 2(a). Therefore, we demonstrated for the measurement of an electromagnetically induced birefringence originating from the EIA-type resonance of the strong probe field in the wavelength-mismatched three-level cascade system.

Finally, we used successfully the measured dispersive LIB signal in Fig. 3(a) for the frequency stabilization of the coupling laser without frequency modulation with long-term, stability below 1 MHz as shown in Fig. 3(b). Furthermore, by stabilizing the frequency of probe laser to the different isotopes of Yb atoms, for example ^{171}Yb , which is a prom-

ising candidate for a future optical lattice clock [7,14], we were able to stabilize the frequency of coupling laser to each stable Yb isotope. The two-photon cooling theory predicts that the minimum temperature of $124\ \mu\text{K}$ for Yb atoms can be reached at the probe and coupling laser detunings of $\delta_p = -\gamma_a/2$ and $\delta_c = -\gamma_b/2$ [5], respectively, and that those conditions can easily be achieved with the current frequency-stabilized laser diodes described in this paper.

In summary, we introduced a Doppler-free two-photon atomic coherence spectroscopy of Yb atoms in a Yb HCL associated with the wavelength-mismatched cascade level configuration. We investigated the transmission spectrum of strong probe field at a fixed one-photon frequency, depending on the detuning of circularly polarized coupling field from a two-photon resonance. We found that the σ_p^+ polarized component, which is coupled to the upper state, exhibits a narrow EIA spectrum, while the σ_p^- polarized component exhibits an EIT spectrum. Numerical solutions of density matrix equations show qualitative agreement with the experimental results. Doppler-free dispersive LIB signal results from the EIA-type resonance were obtained by detecting the Stokes parameter of the probe field, enabling us to stabilize the frequency of coupling laser without frequency modulation. The Doppler-free two-photon atomic coherence spectroscopy introduced in this paper might equally be applied to the alkaline-earth atoms and should be useful for experimental realization of the two-photon cooling theory [5].

This research is supported by the Creative Research Initiatives Program of the Ministry of Science and Technology of Korea. The authors thank H. S. Moon for useful discussions.

-
- [1] K.-J. Boller, A. Imamoglu, and S. E. Harris, Phys. Rev. Lett. **66**, 2593 (1991); A. M. Akulshin, S. Barreiro, and A. Lezama, Phys. Rev. A **57**, 2996 (1998).
- [2] S. Wielandy and A. L. Gaeta, Phys. Rev. Lett. **81**, 3359 (1998).
- [3] A. D. Cronin, R. B. Warrington, S. K. Lamoreaux, and E. N. Fortson, Phys. Rev. Lett. **80**, 3719 (1998).
- [4] F. S. Pavone, G. Bianchini, F. S. Cataliotti, T. W. Hänsch, and M. Inguscio, Opt. Lett. **22**, 736 (1997).
- [5] W. C. Magno, R. L. Cavasso Filho, and F. C. Cruz, Phys. Rev. A **67**, 043407 (2003).
- [6] C. P. Pearman, C. S. Adams, S. G. Cox, P. F. Griffin, D. A. Smith, and I. G. Hughes, J. Phys. B **35**, 5141 (2002); Y. Yoshikawa, T. Umeki, T. Mukae, Y. Torii, and T. Kuga, Appl. Opt. **42**, 6645 (2003); A. Ratnapala, C. J. Vale, A. G. White, M. D. Harvey, N. Heckenberg, and H. Rubinsztein-Dunlop, Opt. Lett. **29**, 2704 (2004).
- [7] C. Y. Park and T. H. Yoon, Phys. Rev. A **68**, 055401 (2003).
- [8] A. K. Patnaik and G. S. Agarwal, Opt. Commun. **199**, 127 (2001); **179**, 97 (2000).
- [9] Y. S. Bai and T. W. Mossberg, Phys. Rev. A **35**, 619 (1987).
- [10] J. R. Boon, E. Zekou, D. McGloin, and M. H. Dunn, Phys. Rev. A **59**, 4675 (1999).
- [11] S. Wielandy and A. L. Gaeta, Phys. Rev. A **58**, 2500 (1998).
- [12] C. Y. Park and T. H. Yoon, Jpn. J. Appl. Phys., Part 2 **42**, L754 (2003); J. I. Kim, C. Y. Park, J. Y. Yeom, E. B. Kim, and T. H. Yoon, Opt. Lett. **28**, 245 (2003).
- [13] T. Loftus, J. R. Bochinski, and T. W. Mossberg, Phys. Rev. A **63**, 053401 (2001).
- [14] S. G. Porsev, A. Derevianko, and E. N. Fortson, Phys. Rev. A **69**, 021403(R) (2004).